

Cite this: *Chem. Sci.*, 2024, 15, 14844

All publication charges for this article have been paid for by the Royal Society of Chemistry

Received 5th May 2024
Accepted 7th August 2024

DOI: 10.1039/d4sc02962c

rsc.li/chemical-science

Visible light-induced halogen-atom transfer by N-heterocyclic carbene-ligated boryl radicals for diastereoselective C(sp³)–C(sp²) bond formation†

Luca Capaldo,[†] Ting Wan,[†] Robin Mulder,^a Jonas Djossou^a and Timothy Noël^{*,a}

Photoinduced halogen-atom transfer (XAT) has rapidly emerged as a programmable approach to generate carbon-centered radical intermediates, mainly relying on silyl and α -aminoalkyl radicals as halogen abstractors. More recently, ligated boryl radicals have also been proposed as effective halogen abstractors under visible-light irradiation. In this study, we describe the use of this approach to enable C(sp³)–C(sp²) bond formation *via* radical addition of carbon-centered radicals generated *via* XAT onto chloroalkynes. Our mechanistic investigation reveals a complex interplay of highly reactive radical intermediates which, under optimized conditions, delivered the targeted vinyl chlorides in excellent yields and *Z*:*E* ratios. Finally, we demonstrated the synthetic value of these products in transition metal-based cross-coupling reactions.

Introduction

Over the past decade, the field of chemistry has experienced a notable expansion in synthetic methodologies, marked by the development of increasingly selective techniques focused on the use of carbon-centered radicals.¹ This advancement is attributed to the accumulation of knowledge over the past century regarding these fleeting intermediates,² coupled with the emergence of gentler approaches for their generation, such as electro-³ and photo-catalysis.⁴ As a specific example, light-mediated halogen-atom transfer (XAT) has emerged as a versatile and controllable method for generating radical intermediates from readily available haloalkanes, predominantly relying on silyl and α -aminoalkyl radicals as halogen abstractors.⁵ In these processes, the excited state of a photocatalyst oxidizes silicon-containing compounds (*e.g.*, supersilane and supersilanol)^{6–8} and amines^{9,10} to unveil the halogen abstractor.

More recently, N-heterocyclic carbene (NHC)-ligated boryl radicals (LBRs) have also been proposed as halogen abstractors under visible-light irradiation.^{11–13} While the mild nucleophilicity of these boron-centered radicals¹⁴ has traditionally been exploited for B–C bond formation,^{15–19} their affinity for halogens can also be utilized for the homolytic activation of a C–X bond, generating carbon-centered radicals *via* XAT (Fig. 1A).^{20–24} We have recently exploited this capability, triggering the reactivity under visible-light irradiation in the presence of an organic photocatalyst to realize C(sp³)–C(sp³) bond formation through a classical Giese-type reaction mechanism (Fig. 1B).^{12,25} In this process, the excited state of the photocatalyst is reductively quenched by an NHC-ligated borane,²⁶ leading to the spontaneous deprotonation and generation of the corresponding LBR.

This species is then responsible for the XAT with a variety of alkyl iodides, producing carbon-centered radicals that subsequently participate in a radical addition step with electron-poor olefins. We wondered whether an LBR-based approach could be viable for C(sp³)–C(sp²) bond formation. Drawing upon the findings from our initial report, we surmised that an effective approach to tackle this challenge would entail exploring a radical addition pathway onto carbon–carbon triple bonds. Unlike acetylenic bromides and sulfones,²⁷ which typically yield alkynylation products *via* a radical addition/ β -fragmentation pathway, their chlorinated analogues retain the halogen atom in the final product, as demonstrated by Hashmi in a seminal work based on HAT.²⁸ Consequently, the resulting vinyl chlorides, which are valuable intermediates for transition metal-based cross-coupling reactions,^{29–31} contain the coveted C(sp³)–C(sp²) bond. This reactivity difference arises from the higher carbon–halogen bond dissociation energy (BDE) for a C–

^aFlow Chemistry Group, Van 't Hoff Institute for Molecular Sciences (HIMS), University of Amsterdam, Science Park 904, 1098 XH Amsterdam, The Netherlands. E-mail: t.noel@uva.nl

^bDepartment of Chemistry, SynCat Lab, Life Sciences and Environmental Sustainability, University of Parma, 43124 Parma, Italy. E-mail: luca.capaldo@unipr.it

^cThe Research Center of Chiral Drugs, Innovation Research Institute of Traditional Chinese Medicine, Shanghai University of Traditional Chinese Medicine, Shanghai 201203, China

† Electronic supplementary information (ESI) available: Procedures, characterization of compounds, spectroscopic data, computational data. See DOI: <https://doi.org/10.1039/d4sc02962c>

‡ These authors contributed equally to this work.

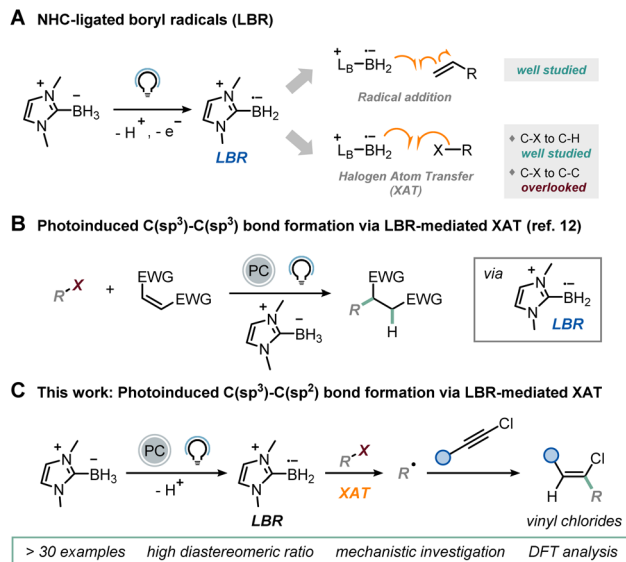


Fig. 1 (A) Use of NHC-ligated boryl radicals (LBRs) in light-mediated synthesis. (B) C(sp³)-C(sp³) bond formation via LBR-mediated XAT. (C) This work: C(sp³)-C(sp²) bond formation via LBR-mediated XAT.

Cl bond, which inhibits the β -fragmentation step.^{28,32} Since this chlorine radical elimination is hindered, we hypothesized that the vinyl radical, deriving from the radical addition of the alkyl radical generated *via* XAT onto the triple bond, could abstract a hydrogen atom from another molecule of NHC-ligated borane, thus initiating a LBR-sustained radical chain mechanism. Given the mild nucleophilicity of LBRs, competitive direct addition onto chloroalkynes should be unfavorable. Herein, we present the realization of this synthetic protocol (Fig. 1C).

Results and discussion

We started our investigations by optimizing the reaction between iodocyclohexane **1a** (2 equiv.) and chloroalkyne **2a** (0.1 mmol) in the presence of ligated borane **B1** (1.2 equiv.). When 4CzIPN (5 mol%) served as the photocatalyst (PC), product **3** was obtained in 26% ¹H NMR yield (Table 1, entry 1) after 12 hours of blue LED irradiation. Employing a more oxidizing acridinium catalyst (Mes-AcrClO₄, $E(\text{PC}^*/\text{PC}_{\text{red}}) = +2.06 \text{ V vs. SCE}$)³³ resulted in similar yields (30%, entry 2), while photocatalysts such as Ru(bpy)₃(PF₆)₂ ($E(\text{PC}^*/\text{PC}_{\text{red}}) = +0.77 \text{ V vs. SCE}$)³⁴ and Eosin Y ($E(\text{PC}^*/\text{PC}_{\text{red}}) = +0.83 \text{ V vs. SCE}$)³⁵ afforded lower NMR yields (entries 3 and 4). This trend can be explained based on the oxidation potential of **B1** ($E_{\text{p}/2} = +0.89 \text{ V vs. SCE}$):³⁶ reductive quenching becomes inefficient with the latter two photocatalysts. The addition of water and a slight increase in the stoichiometry of **B1** (1.5 equiv.) proved beneficial for the transformation (entries 5 and 6), allowing to obtain product **3** in 68% yield. We found that the addition of K₃PO₄ boosted reactivity (6 h *vs.* 12 h), presumably by facilitating deprotonation subsequent to the oxidation of **B1** by PC* to reveal the desired LBR (entry 7). Notably, the product could be obtained with a very good ¹H NMR yield (~80%) even with a reduced loading of 4CzIPN (0.5 mol%, entry 8). Under these conditions, an excellent *Z* : *E* ratio of 92 : 8 was measured (see ESI for additional info†). Control experiments (entries 9 and 10) showed that light, 4CzIPN and **B1** are all necessary for initiating the desired reactivity. Moreover, when we tried to execute the same transformation with silyl radicals or α -aminoalkyl radicals, we could not obtain product **3** in satisfactory yields (Section 9 in the ESI†).

With the optimized conditions in hand (Table 1, entry 8), we proceeded to explore the scope of the transformation (Fig. 2).

Table 1 Optimization of reaction conditions

Entry	Variation from conditions	Yield ^a (%)
1	None	26
2	Mes-AcrClO ₄ instead of 4CzIPN	30
3	Ru(bpy) ₃ (PF ₆) ₂ instead of 4CzIPN	10
4	Eosin Y instead of 4CzIPN	14
5	As entry 1, MeCN/H ₂ O 9 : 1 instead of MeCN	56
6	As entry 5, 1a : 2a : B1 2 : 1 : 1.5	68
7	As entry 6, 4CzIPN (2 mol%), K ₃ PO ₄ (0.5 equiv.), 6 h	80
8	As entry 7, 4CzIPN (0.5 mol%), 6 h	82 (<i>Z</i> : <i>E</i> 92 : 8)^b; 73^c
9	As entry 8, no PC, no B1 or no light	n.d.
10	As entry 8, Δ (80 °C, dark)	n.d.

^a Yields were determined *via* ¹H-NMR by using CH₂Br₂ as external standard. ^b The *Z* : *E*-ratio was determined *via* ¹H-NMR of the reaction crude.

^c Yield of the isolated product. n.d.: not detected.



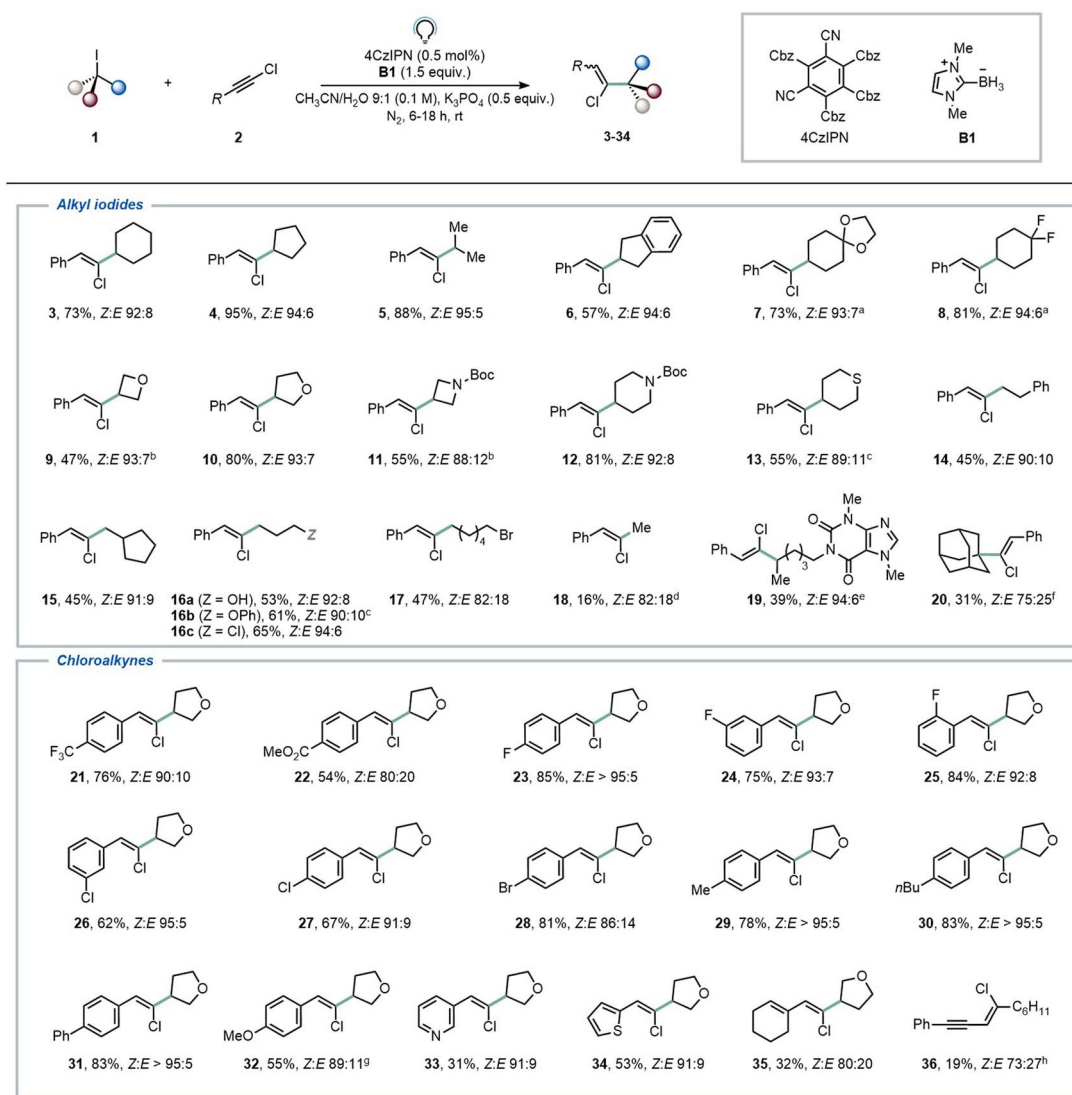


Fig. 2 Scope of the transformation. Reported yields of compounds reflect values obtained after purification via column chromatography; displayed Z : E ratios were determined via ¹H-NMR of the reaction crude. Major isomers (Z) are shown. For secondary organic halides (GP3 in the ESI†): **2** (0.5 mmol), **1** (2 equiv.), **B1** (1.5 equiv.), K₃PO₄ (0.5 equiv.) in CH₃CN/H₂O 9 : 1 (5 mL) in the presence of 4CzIPN (0.5 mol%), 6 h. For primary organic halides (GP4 in the ESI†): **2** (1.5 equiv.), **1** (0.5 mmol), **B1** (1.5 equiv.), K₃PO₄ (0.5 equiv.) in CH₃CN/H₂O 9 : 1 (5 mL) in the presence of 4CzIPN (0.5 mol%), 18 h. Solutions were bubbled with N₂ (5 min) prior to irradiation (40 W Kessil lamp, λ = 456 nm). ^a**1** was used in 1.5 equiv. ^bReaction time: 8 h. ^cReaction time: 16 h. ^d10 equivalents of methyl iodide were used. ^e0.5 mmol of **1** and 2 equiv., of **2** were used. ^f0.5 mmol of **1** and 1.2 equiv., of **2** were used. ^g34% of the corresponding alkyne (**32'**) was isolated as well. ^hReaction carried out on 0.1 mmol scale.

First, various secondary halides were subjected to the reaction conditions, revealing that both cyclic and acyclic iodoalkanes delivered the anticipated products in good to excellent yields and diastereomeric ratios (**3–13**, 47–95%). Both acetal and CF₂ moieties were successfully tolerated under the reaction conditions, yielding the desired products (**7–8**, 73–81%). Saturated N- and S-containing heterocycles were also well accommodated, encompassing pharmaceutically relevant azetidine and piperidine derivatives (**9–13**, 47–81%). Subsequently, we explored the option of employing primary iodides under our reaction conditions. This necessitated slight modifications to the reaction conditions, as we found in our previous report,¹² including a different organic halide/chloroalkyne ratio (**1** : **2** 1 : 1.5) and

prolonged light exposure (18 h vs. 6 h). With these conditions, complete conversion of the halide was observed, affording compounds **14–18** in satisfactory yields (45–65%). Intriguingly, our approach proved chemoselective towards C–I bonds (see compound **17**) leaving C–Br unaffected. This shows complementary reactivity compared to the more common XAT manifolds based on silyl and α-aminoalkyl radicals. Also methylation could be realized using our methodology (**18**). A caffeine derivative could be functionalized as well, albeit in modest yield (**19**, 39%). One tertiary iodide also proved to be an effective coupling partner, yielding the desired compound in a synthetically useful yield and modest diastereoselectivity (**20**, 31%, Z : E 75 : 25). However, alkyl bromides continued to present



We then shifted our attention towards elucidating the mechanism to gain a more comprehensive understanding of the reaction. Our initial hypothesis (Fig. 3A) proposed that reductive quenching of the photocatalyst excited state would lead, upon base-aided deprotonation, to the crucial ligated boryl radical (**I'**). This species would subsequently engage with



organohalides *via* XAT to generate a carbon-centered radical (**II'**), which would then be readily intercepted by the chloroalkyne (**2**). The regioselectivity of this step is known to be influenced by both thermodynamic and kinetic factors.²⁸ The resulting vinyl radical (**III'**) is expected to exhibit high reactivity and would abstract a hydrogen atom from a molecule of **B1**, yielding the anticipated vinyl chloride and regenerating the LBR, thereby initiating a radical chain mechanism.

To further investigate the occurrence of a radical chain mechanism, we conducted deuteration experiments (Fig. 3B). When the model reaction was performed in the presence of **B1-d₃** instead of **B1**, complete incorporation of deuterium was observed, strongly suggesting the operation of a radical chain mechanism. In contrast, when deuterated solvent was used (CD₃CN/D₂O 9:1), no deuterium atom was incorporated into the product. Additionally, we measured the Kinetic Isotope Effect (KIE) of the reaction using the parallel reaction method³⁷ and found a value of 1.2 (see Section 9 in the ESI†), which suggests that the halogen atom transfer might be limiting the rate of the reaction.

To get further insights, we conducted a computational investigation aimed at modelling the entire reaction profile between substrates **1h** and **2a**, simulating all key steps including XAT, radical addition, and HAT. We adopted Density Functional Theory (DFT) at the (U)ωB97xD/def2TZVP level of theory to optimize the relevant stationary points, also including the effect of the solvent (CH₃CN) using an implicit model (Fig. 3C). Initially, we considered the reaction between the LBR (**I'**) and **1a** *via* **TS1** ($\Delta G^\ddagger = +9.8 \text{ kcal mol}^{-1}$) to afford alkyl radical **II'**, which is then trapped by chloroalkyne **2a** *via* **TS2** ($\Delta G^\ddagger = +15.9 \text{ kcal mol}^{-1}$). Vinyl radicals are known to adopt either a linear or a bent geometry, depending on the substituent attached to the carbon bearing the unpaired electron. Our DFT analysis confirmed that when this substituent is a π -type group (*e.g.*, a phenyl ring), the vinyl radical adopts a linear geometry, thus suggesting that stereochemical control does not occur in the radical addition step to yield **III'**.^{38–40} Moreover, it has been reported³⁹ that the barrier for inversion of bent vinyl radicals is typically low, further diminishing the likelihood of the radical addition step being the key determinant of the observed stereoselectivity. From **III'**, the targeted vinyl chloride **10** is formed through reaction with NHC-ligated borane **B1** *via* **TS3_Z** ($\Delta G^\ddagger = +14.6 \text{ kcal mol}^{-1}$) or **TS3_E** ($\Delta G^\ddagger = +16.1 \text{ kcal mol}^{-1}$). We propose that *Z*-diastereoselectivity originates in this step, despite the marginal thermodynamic ($\Delta\Delta G_{E-Z} = 1.5 \text{ kcal mol}^{-1}$) and kinetic ($\Delta\Delta G^\ddagger = +1.5 \text{ kcal mol}^{-1}$) driving forces. It is crucial to note that due to the conjugated structure of the prepared vinyl chlorides, triplet-triplet sensitization might be an underlying process. While we did observe photoisomerization, it is noteworthy that this process was identified to be comparatively slower than the formation of the vinyl chloride itself. Consequently, one can halt the reaction before photoisomerization occurs (see Section 9 in the ESI†).^{41,42} A quantum yield for vinyl chloride formation was determined to be 10% *via* ferrioxalate actinometry. Such a modest value is consistent with a process being supported by either short-lived radical chain propagations or an inefficient initiation process.⁴³

Finally, we demonstrated the synthetic value of the synthesized vinyl chlorides (Fig. 3D). The chlorine atom in **Z-12** could be readily substituted with cyanide under Pd-catalysis to afford product **37** in 50% yield. Similarly, the same substrate exhibited compatibility for a nickel-mediated Kumada–Corriu-type coupling (**38**, 44%) and was also effective in the Pd-catalyzed Suzuki–Miyaura coupling (**39**, 91%).

Conclusions

In summary, this work elucidates the effective utilization of NHC-ligated boryl radicals for promoting the formation of C(sp³)–C(sp²) bonds under visible light irradiation through XAT. The boron-centered radicals served as halogen abstractors for a diverse array of organoiodides, generating carbon-centered radicals that readily underwent radical addition with chloroalkynes, resulting in the formation of synthetically valuable vinyl chlorides. Despite being previously reported by Hashmi *via* HAT,²⁸ the current methodology offers several advantages, including reduced excess of the alkyl coupling partner, broader substrate scope, minimal photocatalyst loading, and improved diastereoselectivity. While the reduced nucleophilicity of the ligated boryl radical limits the activation of alkyl bromides, it concurrently enhances selectivity by discouraging direct addition to the triple bond. This study represents the first protocol employing XAT for establishing a C(sp³)–C(sp²) bond through a radical addition mechanism and demonstrates the synthetic value of ligated boryl radicals.

Data availability

The data supporting this article have been included as part of the ESI.†

Author contributions

L. C.: conceptualization, investigation, writing – original draft, writing – review & editing, project administration. T. W. & R. M.: investigation, data curation, writing – review & editing. T. N.: supervision, writing – review & editing.

Conflicts of interest

There are no conflicts to declare.

Acknowledgements

L. C. acknowledges the framework of the COMP-R Initiatives, funded by the ‘Departments of Excellence’ programs of the Italian Ministry for University and Research (MUR, 2023–2027). We acknowledge the CINECA award under the ISCRA initiative, for the availability of high-performance computing resources and support. T.W. has received support from the China Scholarship Council (CSC) for her PhD studies. We also received support from the European Union H2020 under the ERC Consolidator Grant (FlowHAT, No. 101044355, T. N.) and MSCA ITN (GreenDigiPharma, No. 101073089, J. D. and T. N.).



References

- 1 S. Z. Zard, Radicals in Action: A Festival of Radical Transformations, *Org. Lett.*, 2017, **19**, 1257–1269.
- 2 A. Studer and D. P. Curran, Catalysis of Radical Reactions: A Radical Chemistry Perspective, *Angew. Chem., Int. Ed.*, 2016, **55**, 58–102.
- 3 L. F. T. Novaes, J. Liu, Y. Shen, L. Lu, J. M. Meinhardt and S. Lin, Electrocatalysis as an enabling technology for organic synthesis, *Chem. Soc. Rev.*, 2021, **50**, 7941–8002.
- 4 S. Crespi and M. Fagnoni, Generation of Alkyl Radicals: From the Tyranny of Tin to the Photon Democracy, *Chem. Rev.*, 2020, **120**, 9790–9833.
- 5 F. Julia, T. Constantin and D. Leonori, Applications of Halogen-Atom Transfer (XAT) for the Generation of Carbon Radicals in Synthetic Photochemistry and Photocatalysis, *Chem. Rev.*, 2022, **122**, 2292–2352.
- 6 P. Zhang, C. C. Le and D. W. MacMillan, Silyl Radical Activation of Alkyl Halides in Metallaphotoredox Catalysis: A Unique Pathway for Cross-Electrophile Coupling, *J. Am. Chem. Soc.*, 2016, **138**, 8084–8087.
- 7 C. Le, T. Q. Chen, T. Liang, P. Zhang and D. W. C. MacMillan, A radical approach to the copper oxidative addition problem: Trifluoromethylation of bromoarenes, *Science*, 2018, **360**, 1010–1014.
- 8 A. ElMarrouni, C. B. Ritts and J. Balsells, Silyl-mediated photoredox-catalyzed Giese reaction: addition of non-activated alkyl bromides, *Chem. Sci.*, 2018, **9**, 6639–6646.
- 9 V. S. Kostromitin, A. O. Sorokin, V. V. Levin and A. D. Dilman, Aminals as powerful XAT-reagents: activation of fluorinated alkyl chlorides, *Chem. Sci.*, 2023, **14**, 3229–3234.
- 10 T. Constantin, M. Zanini, A. Regni, N. S. Sheikh, F. Julia and D. Leonori, Aminoalkyl radicals as halogen-atom transfer agents for activation of alkyl and aryl halides, *Science*, 2020, **367**, 1021–1026.
- 11 V. I. Supranovich, V. V. Levin, M. I. Struchkova, A. A. Korlyukov and A. D. Dilman, Radical Silyldifluoromethylation of Electron-Deficient Alkenes, *Org. Lett.*, 2017, **19**, 3215–3218.
- 12 T. Wan, L. Capaldo, D. Ravelli, W. Vitullo, F. J. de Zwart, B. de Bruin and T. Noël, Photoinduced Halogen-Atom Transfer by N-Heterocyclic Carbene-Ligated Boryl Radicals for C(sp³)–C(sp³) Bond Formation, *J. Am. Chem. Soc.*, 2023, **145**, 991–999.
- 13 T. Wan, L. W. Ciszewski, D. Ravelli and L. Capaldo, Photoinduced Intermolecular Radical Hydroalkylation of Olefins via Ligated Boryl Radicals-Mediated Halogen Atom Transfer, *Org. Lett.*, 2024, **26**, 5839–5843.
- 14 L. Capaldo, T. Noël and D. Ravelli, Photocatalytic generation of ligated boryl radicals from tertiary amine-borane complexes: An emerging tool in organic synthesis, *Chem. Catal.*, 2022, **2**, 957–966.
- 15 T. Taniguchi, Advances in chemistry of N-heterocyclic carbene boryl radicals, *Chem. Soc. Rev.*, 2021, **50**, 8995–9021.
- 16 T. Y. Peng, F. L. Zhang and Y. F. Wang, Lewis Base-Boryl Radicals Enabled Borylation Reactions and Selective Activation of Carbon-Heteroatom Bonds, *Acc. Chem. Res.*, 2023, **56**, 169–186.
- 17 S. C. Ren, F. L. Zhang, J. Qi, Y. S. Huang, A. Q. Xu, H. Y. Yan and Y. F. Wang, Radical Borylation/Cyclization Cascade of 1,6-Enynes for the Synthesis of Boron-Handled Hetero- and Carbocycles, *J. Am. Chem. Soc.*, 2017, **139**, 6050–6053.
- 18 J. Qi, F. L. Zhang, J. K. Jin, Q. Zhao, B. Li, L. X. Liu and Y. F. Wang, New Radical Borylation Pathways for Organoboron Synthesis Enabled by Photoredox Catalysis, *Angew. Chem., Int. Ed.*, 2020, **59**, 12876–12884.
- 19 Q. Zhao, B. Li, X. Zhou, Z. Wang, F. L. Zhang, Y. Li, X. Zhou, Y. Fu and Y. F. Wang, Boryl Radicals Enabled a Three-Step Sequence to Assemble All-Carbon Quaternary Centers from Activated Trichloromethyl Groups, *J. Am. Chem. Soc.*, 2022, **144**, 15275–15285.
- 20 S. H. Ueng, L. Fensterbank, E. Lacote, M. Malacria and D. P. Curran, Radical reductions of alkyl halides bearing electron withdrawing groups with N-heterocyclic carbene boranes, *Org. Biomol. Chem.*, 2011, **9**, 3415–3420.
- 21 X. Pan, E. Lacote, J. Lalevee and D. P. Curran, Polarity reversal catalysis in radical reductions of halides by N-heterocyclic carbene boranes, *J. Am. Chem. Soc.*, 2012, **134**, 5669–5674.
- 22 S. H. Ueng, A. Solov'yev, X. Yuan, S. J. Geib, L. Fensterbank, E. Lacote, M. Malacria, M. Newcomb, J. C. Walton and D. P. Curran, N-heterocyclic carbene boryl radicals: a new class of boron-centered radical, *J. Am. Chem. Soc.*, 2009, **131**, 11256–11262.
- 23 S. H. Ueng, M. M. Brahmi, E. Derat, L. Fensterbank, E. Lacote, M. Malacria and D. P. Curran, Complexes of borane and N-heterocyclic carbenes: a new class of radical hydrogen atom donor, *J. Am. Chem. Soc.*, 2008, **130**, 10082–10083.
- 24 D. P. Curran, A. Solov'yev, M. Makhlof Brahmi, L. Fensterbank, M. Malacria and E. Lacote, Synthesis and reactions of N-heterocyclic carbene boranes, *Angew. Chem., Int. Ed.*, 2011, **50**, 10294–10317.
- 25 B. Giese, Formation of CC Bonds by Addition of Free Radicals to Alkenes, *Angew. Chem., Int. Ed.*, 2003, **22**, 753–764.
- 26 L. Capaldo, *Encyclopedia of Reagents for Organic Synthesis*, 2024, pp. 1–8, DOI: [10.1002/047084289X.rm02566](https://doi.org/10.1002/047084289X.rm02566).
- 27 D. Ge, X. Wang and X.-Q. Chu, SOMOphilic alkynylation using acetylenic sulfones as functional reagents, *Org. Chem. Front.*, 2021, **8**, 5145–5164.
- 28 T. Adak, M. Hoffmann, S. Witzel, M. Rudolph, A. Dreuw and A. S. K. Hashmi, Visible Light-Enabled sp³–C–H Functionalization with Chloro- and Bromoalkynes: Chemoselective Route to Vinylchlorides or Alkynes, *Chem.–Eur. J.*, 2020, **26**, 15573–15580.
- 29 L. Zhang, Modular Synthesis of α -Substituted Alkenyl Acetals by a Palladium-Catalyzed Suzuki Reaction of α -Haloalkenyl Acetals with Organoboranes, *Synlett*, 2020, **32**, 723–727.
- 30 Z. Tan and E. Negishi, Widely applicable Pd-catalyzed trans-selective monoalkylation of unactivated 1,1-dichloro-1-alkenes and Pd-catalyzed second substitution for the



- selective synthesis of E or Z trisubstituted alkenes, *Angew. Chem. Int. Ed. Engl.*, 2006, **45**, 762–765.
- 31 L. Huo, X. Li, Y. Zhao, L. Li and L. Chu, Site- and Stereoselective Synthesis of Alkenyl Chlorides by Dual Functionalization of Internal Alkynes *via* Photoredox/Nickel Catalysis, *J. Am. Chem. Soc.*, 2023, **145**, 9876–9885.
 - 32 L. Capaldo and D. Ravelli, Decatungstate as Direct Hydrogen Atom Transfer Photocatalyst for SOMOphilic Alkynylation, *Org. Lett.*, 2021, **23**, 2243–2247.
 - 33 I. A. MacKenzie, L. Wang, N. P. R. Onuska, O. F. Williams, K. Begam, A. M. Moran, B. D. Dunietz and D. A. Nicewicz, Discovery and characterization of an acridine radical photoreductant, *Nature*, 2020, **580**, 76–80.
 - 34 C. Creutz and N. Sutin, Electron-transfer reactions of excited states. Reductive quenching of the tris(2,2'-bipyridine) ruthenium(II) luminescence, *Inorg. Chem.*, 2002, **15**, 496–499.
 - 35 T. Lazarides, T. McCormick, P. Du, G. Luo, B. Lindley and R. Eisenberg, Making hydrogen from water using a homogeneous system without noble metals, *J. Am. Chem. Soc.*, 2009, **131**, 9192–9194.
 - 36 G. Lei, M. Xu, R. Chang, I. Funes-Ardoiz and J. Ye, Hydroalkylation of Unactivated Olefins *via* Visible-Light-Driven Dual Hydrogen Atom Transfer Catalysis, *J. Am. Chem. Soc.*, 2021, **143**, 11251–11261.
 - 37 E. M. Simmons and J. F. Hartwig, On the interpretation of deuterium kinetic isotope effects in C-H bond functionalizations by transition-metal complexes, *Angew. Chem., Int. Ed.*, 2012, **51**, 3066–3072.
 - 38 H. Rubin and H. Fischer, The Addition of tert-Butyl (Me₃C•) and (tert-Butoxy)carbonylmethyl (Me₃CO₂C•CH₂) radicals to alkynes in solution studied by ESR spectroscopy, *Helv. Chim. Acta*, 2004, **79**, 1670–1682.
 - 39 C. Galli, A. Guarnieri, H. Koch, P. Mencarelli and Z. Rappoport, Effect of Substituents on the Structure of the Vinyl Radical: Calculations and Experiments, *J. Org. Chem.*, 1997, **62**, 4072–4077.
 - 40 L. Bonazzola, S. Fenistein and R. Marx, Electronic structure of α -substituted vinyl radicals, *Mol. Phys.*, 2006, **22**, 689–695.
 - 41 X. J. Wei, W. Boon, V. Hessel and T. Noel, Visible-Light Photocatalytic Decarboxylation of α,β -Unsaturated Carboxylic Acids: Facile Access to Stereoselective Difluoromethylated Styrenes in Batch and Flow, *ACS Catal.*, 2017, **7**, 7136–7140.
 - 42 N. J. Straathof, S. E. Cramer, V. Hessel and T. Noel, Practical Photocatalytic Trifluoromethylation and Hydrotrifluoromethylation of Styrenes in Batch and Flow, *Angew. Chem., Int. Ed.*, 2016, **55**, 15549–15553.
 - 43 S. P. Pitre, C. D. McTiernan, W. Vine, R. DiPucchio, M. Grenier and J. C. Scaiano, Visible-Light Actinometry and Intermittent Illumination as Convenient Tools to Study Ru(bpy)₃Cl₂ Mediated Photoredox Transformations, *Sci. Rep.*, 2015, **5**, 16397.

